environmental microbiology

Environmental Microbiology (2010) **12**(7), 1842–1854 doi:10.1111/j.1462-2920.2010.02189.x

The effect of nutrient deposition on bacterial communities in Arctic tundra soil

Barbara J. Campbell,[1]* Shawn W. Polson,[2,3] Thomas E. Hanson,[1,3] Michelle C. Mack[4] and Edward A. G. Schuur[4]

[1]*College of Earth, Ocean, and Environment, University of Delaware, Lewes, DE 19958, USA.*

[2]*Department of Plant and Soil Sciences and* [3]*Delaware Biotechnology Institute, University of Delaware, Newark, DE 19711, USA.*

[4]*Department of Botany, University of Florida, Gainesville, FL 32611, USA.*

Summary

The microbial communities of high-latitude ecosystems are expected to experience rapid changes over the next century due to climate warming and increased deposition of reactive nitrogen, changes that will likely affect microbial community structure and function. In moist acidic tundra (MAT) soils on the North Slope of the Brooks Range, Alaska, substantial losses of C and N were previously observed after long-term nutrient additions. To analyse the role of microbial communities in these losses, we utilized 16S rRNA gene tag pyrosequencing coupled with community-level physiological profiling to describe changes in MAT bacterial communities after short- and long-term nutrient fertilization in four sets of paired control and fertilized MAT soil samples. Bacterial diversity was lower in long-term fertilized plots. The *Acidobacteria* were one of the most abundant phyla in all soils and distinct differences were noted in the distributions of *Acidobacteria* subgroups between mineral and organic soil layers that were also affected by fertilization. In addition, *Alpha-* and *Gammaproteobacteria* were more abundant in long-term fertilized samples compared with control soils. The dramatic increase in sequences within the *Gammaproteobacteria* identified as *Dyella* spp. (order *Xanthomonadales*) in the long-term fertilized samples was confirmed by quantitative PCR (qPCR) in several samples. Long-term fertilization was also correlated with shifts in the utilization of specific substrates by microbes present in the soils. The combined data indicate that long-term fertilization resulted in a significant change in microbial community structure and function linked to changes in carbon and nitrogen availability and shifts in above-ground plant communities.

Received 5 November, 2007; accepted 12 January, 2010. *For correspondence. E-mail bjc@udel.edu; Tel. (+1) 302 645 4304; Fax (+1) 302 645 4007.

Introduction

Approximately one-third of the total global soil C pool is stored below ground as organic matter in high-latitude ecosystems (Post *et al.*, 1982; Dixon *et al.*, 1994; Houghton, 1996; Goulden *et al.*, 1998). However, surprisingly little is known about the microbial communities that utilize this large C pool in these ecosystems. Two prior studies found somewhat similar microbial community structures in Arctic tundra soils where *Acidobacteria* dominated acidic soils and tussock tundra and *Proteobacteria* dominated higher pH soils and shrub-covered tundra (Neufeld and Mohn, 2005; Wallenstein *et al.*, 2007). These phylum-level differences reflect variations in pH, soil type, organic matter composition and plant cover. These and other authors hypothesize that plant type controls the community composition of the soils (Wardle *et al.*, 1997; Wallenstein *et al.*, 2007). However, studies indicate that pH and possibly mineralizable carbon are more important in controlling microbial community structure in diverse soils (Neufeld and Mohn, 2005; Fierer and Jackson, 2006; Jangid *et al.*, 2008).

One way to test these hypotheses is to examine the structure of microbial communities in manipulated soils. The composition and structure of disturbed or fertilized microbial soil communities substantially differs from control soils (Mccaig *et al.*, 1999; Deslippe *et al.*, 2005; Neufeld and Mohn, 2005; Ge *et al.*, 2008; Jangid *et al.*, 2008). For instance, a disturbed Arctic soil sample from Cape Dyer, Canada was significantly less diverse than other Arctic soils and contained almost 16% of a single sequence, a *Gammaproteobacterium*, with the highest identity to members of the *Xanthomonadales* (Neufeld and Mohn, 2005). Inorganic nutrient fertilization of cropland and pasture soils in Georgia, USA significantly decreased the diversity of and changed the composition of a number of bacterial phyla, including the *Acidobacteria*, *Bacteroidetes*, *Firmicutes*, *Planctomycetes*, and the beta- and gammaproteobacterial classes (Jangid *et al.*,

Table 1. Key to sample codes used in subsequent tables and figures and number of sequences analysed per sample after trimming.

				No. of sequences	
Code	Duration	Treatment	Soil Layer	B read	FLX
NCO	6 weeks (New)	None (Control)	Organic	3315	1227
NFO	6 weeks (New)	Fertilized	Organic	2431	938
NCM	6 weeks (New)	None (Control)	Mineral	1721	
NFM	6 weeks (New)	Fertilized	Mineral	1999	
HCO	24 years (Historic)	None (Control)	Organic	1801	811
HFO	24 years (Historic)	Fertilized	Organic	1517	1578
HCM	24 years (Historic)	None (Control)	Mineral	1839	
HFM	24 years (Historic)	Fertilized	Mineral	1732	

2008). Interestingly, the most abundant operational taxonomic unit (OTU) from this inorganic fertilizer-amended cropland was also a member of the *Xanthomonadales* (Jangid *et al.*, 2008).

How altered nutrient availability alters high-latitude tundra microbial communities and the ecosystem processes they mediate, such as C or N cycling, is less clear. Previous studies documented that nitrogen and phosphorous fertilization caused increased plant productivity and shrub dominance in moist acidic tundra (MAT) ecosystems (Chapin and Shaver, 1988; Chapin *et al.*, 1995; Shaver *et al.*, 2001). Shrub soils differ from tussock tundra with increased recalcitrant forms of organic matter and increased nitrogen availability (Weintraub and Schimel, 2005; Wallenstein *et al.*, 2007). Additionally, long-term (> 20 years) nutrient additions to MAT at Toolik Lake was correlated with a net ecosystem loss of almost 2 kg C m^{-2}, primarily from deep mineral soil layers (Mack *et al.*, 2004; Nowinski *et al.*, 2008). The corresponding increased production in the fertilized relative to the control treatment suggested that nutrient fertilization stimulated microbial decomposition of soil organic matter resulting in the large C loss. Therefore, we and others hypothesize that N availability might promote microbial growth and respiration in turn decreasing soil C storage (Neff and Hooper, 2002; Schimel and Weintraub, 2003; Hobbie and Gough, 2004; Mack *et al.*, 2004).

This study sought to document changes in microbial community structure and function in MAT soils subject to nutrient fertilization at the Toolik Lake Long-term Experimental Research station in northern Alaska. This study combines 16S rRNA gene tag sequencing (Sogin *et al.*, 2006) with community-level physiological profiling (CLPP) (Miguel *et al.*, 2007) in controlled MAT manipulation experiments to test the hypothesis that nutrient amendments result in altered community structure and function that are correlated with C and N losses previously documented in the same plots (Mack *et al.*, 2004). MAT soil microbial communities were sampled after short-term (6 weeks) and long-term (24 years) N and P addition experiments. The increased abundance of a specific bacterial group from long-term fertilized plots was checked by quantitative PCR (qPCR) and further demonstrated in additional soil samples that had been fertilized for 16 years. The results indicated that community structure shifts occurred in organic soils subjected to long-term fertilization and that the long-term fertilized community displayed altered substrate utilization patterns, consistent with the hypothesis.

Results

Microbial community structure and diversity were analysed in MAT plots 6 weeks after an initial fertilization (short-term, new) and after 24 years of annual fertilization (long-term, historic) with paired control and fertilized samples from each experiment. Mineral and organic horizons were separated from each core and DNA was extracted from each horizon/core separately to prepare 16S rRNA gene tag sequence libraries. The samples were given three-letter codes that will be used to describe them throughout this article (Table 1).

Two pyrosequencing techniques were used to produce sequence libraries. A total of 35 055 reads, with an average length of 110 ± 15 bp, were collected from the eight samples by 454 GS-20 pyrosequencing (Table 1). After trimming of the primer sequence and screening, a total of 16 355 B-primer reads were analysed (average = 99 ± 6 bp). The organic layers from four replicate cores were analysed on a 454 GS-FLX pyrosequencer, generating 12 440 sequences with an average length of 122 ± 78 bp, with 6939 of these reads < 70 bp in length. Following trimming and screening, 4554 sequences averaging 202 ± 12 bp in length were used for subsequent analyses.

Bacterial OTU richness and diversity in MAT soils

Tag sequences were initially clustered into OTUs using the furthest neighbour clustering algorithm in DOTUR with distances of 0.03, 0.05 and 0.10 to define OTUs, values commonly used in 16S rRNA gene pyrosequencing and

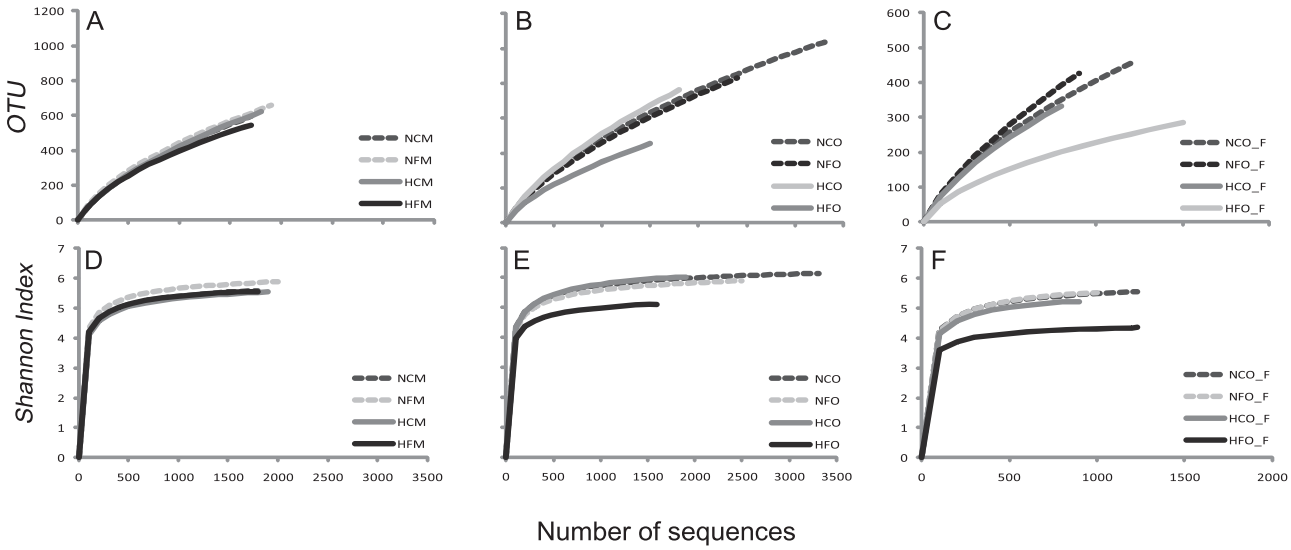

Fig. 1. Diversity of moist acidic tundra (MAT) soils. Rarefaction analysis (A, B and C) and Shannon indices (C, D and E) of 16S rRNA gene GS-20 (B read) sequences from control and fertilized organic (B and E) and mineral (A and D) soil samples based on 97% similarity. Codes for each sample are indicated in Table 1. GS-FLX organic data are in (C) and (F), for the rarefaction and Shannon indices respectively. Note the change in scale in (C) and (F). The letter F indicates GS-FLX sequences.

other 16S rRNA gene studies (Fulthorpe *et al*., 2008; Mckenna *et al*., 2008). This analysis grouped the sequences into 9897, 5625, 4257 or 2627 OTUs at distances of 0.00, 0.03, 0.05 or 0.10 respectively.

While 454 accuracy has improved in recent iterations, GS-20 pyrosequencing is a relatively error-prone technique and sequencing errors can cause overestimation of OTUs using the farthest neighbour algorithm (Huse *et al*., 2007). Other methods, including averaging, are suggested to accurately assess diversity with this technology (Quince *et al*., 2009). Calculations based on the average linkage method (Unweighted Pair Group Method with Arithmetic mean, UPMGA) resulted in 80–85% the number of OTUs produced via DOTUR (Schloss and Handelsman, 2005; Schloss *et al*., 2009) with furthest neighbour distances of 0.03 and 0.05, but were 99% of the value at the 0.10 distance (data not shown). Since the values were not very different, we chose to base our OTU definitions on the furthest neighbour definition. We focus here on the 0.05 distance level because the diversity patterns were similar at all distances, albeit somewhat more pronounced with increasing distance. We also chose the 0.05 farthest neighbour distance calculation as that which best approximated the generally accepted 0.03 cut-off for the entire 16S rRNA gene at the species level (Stackebrandt and Goebel, 1994). Furthest neighbour distances were calculated from the full-length and short V3 regions of the 16S rRNA genes from more than 50 different known species/strains closely related to the sequences found in this study. The 0.05 distance cut-off gave the closest results to the previously generally accepted 0.03 distance for defining a species (Stackebrandt and Goebel, 1994) and our estimates based on the entire 16S rRNA gene averaged across all the tested species/strains (data not shown).

Rarefaction curves of individual sample OTUs versus numbers of sequences analysed did not plateau (Fig. 1A and B, Fig. S1) even with over 3000 GS-20 sequences from a single sample, suggesting that MAT soils contain extensive microbial diversity. In contrast, the Shannon index of community diversity stabilized within a relatively small number of sequences (Fig. 1D and E, Fig. S2) suggesting that representative samples were obtained for estimating Shannon indices. Similar patterns were observed in GS-FLX (Fig. 1C and F, Figs S1 and S2) sequencing data sets obtained from replicate cores of organic soil layers.

Only the historic fertilized organic (HFO) samples displayed distinct decreases in the number of OTUs (Fig. 1A) when equal numbers of GS-20 or GS-FLX sequences (Fig. 1C) were considered and this decrease was observed at all distances used (Fig. S1). The HFO GS-20 library contained between 67% and 75% of the number of OTUs relative to the other three organic samples (HCO, NCO and NFO) at the 0.05 distance (range of 57–61% for the GS-FLX data set). The HFO sample also displayed distinctly lower Shannon index values, averaging 87% and 80% of the other three organic samples at the 0.05 distance for the GS-20 and GS-FLX data sets respectively (Fig. 1). Lower amounts of diversity were also observed in the HFO samples in Rao diversity coefficient calculations, which utilize both phylotype abundance and dissimilarity (data not shown) (Pavoine *et al*., 2004; Eckburg *et al*., 2005). The HFO samples were significantly less diverse than the organic samples from the control and newly

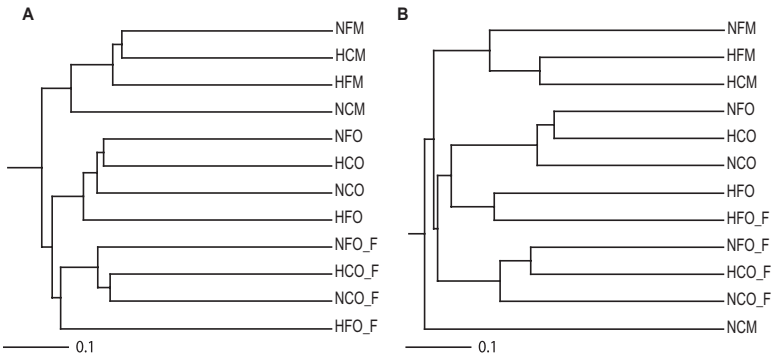

Fig. 2. MAT bacterial community membership similarities (Sorclass, A) and community structure (θ_{YC}, B) similarities between samples. Values are based on 0.05 distances. Abbreviations listed in Table 1.

fertilized plots (*t*-test, $P < 0.001$). The non-parametric diversity estimators, Chao1 and ACE, also demonstrated that the richness of the HFO and HCO communities were different, based on a 0.05 distance (Fig. S3).

Community membership and structure similarities in MAT soils

Two approaches were used to identify between sample (organic versus mineral), between method (GS-20 versus GS-FLX), and between treatment (control versus fertilized) differences in microbial community membership and structure (Schloss and Handelsman, 2005; 2006a; Schloss *et al*., 2009). First, both the Sorenson similarity based on observed richness (Sorclass) and Jaccard similarity based on Chao1 shared OTUs (Jest) coefficients were calculated at distances of 0.03, 0.05 and 0.10 to estimate similarities based on shared OTU presence. The resulting dendrograms gave nearly identical topologies; only the Sorclass dendrogram based on a 0.05 distance is presented (Fig. 2A). There were two major clusters; the mineral group was separated from the organic group, suggesting clear distinctions in the types of OTUs present in the two types of samples. Within the organic group, the samples clustered according to the sequencing method (GS-20 versus GS-FLX), but in both cases, the long-term fertilized samples were clearly separated from the other organic samples suggesting the HFO sample had a distinct pattern of OTU distribution.

Second, Theta – Yue and Clayton similarity coefficient (θ_{YC}) and other coefficients of community structure (Jabund, Sorabund) that account for OTU abundance (Schloss and Handelsman, 2006a; Schloss *et al*., 2009) were calculated based on the same 0.03, 0.05 and 0.10 distances used above. A representative θ_{YC} dendrogram, based on an OTU distance of 0.05, shows the non-parametric relationship between the samples (Fig. 2B). Dendrograms of other measures of community structure (Jabund, Sorabund) and with other distances (0.03, 0.10) were nearly identical in topology (data not shown). θ_{YC} index comparisons via clustering identified two major clusters and one outlier (NCM). As with the methods above, organic and mineral samples other than NCM were placed in distinct clades. In contrast to the community membership relationships based on shared OTUs, the two long-term fertilized organic samples were grouped in this analysis as a distinct clade rather than being deep branches in their respective clades.

Differences in community composition in MAT soils

All sequences were assigned to taxonomic ranks in the Ribosomal Database Project hierarchy to provide some information about the identity of the sequences contributing to the quantitative differences between samples reported above. Out of the total of 20 909 sequences, 13 767 (66%) were classified at the phylum level with 70% confidence or greater using the naïve Bayesian classifier (Wang *et al*., 2007). This analysis indicated that MAT soil samples were dominated by the *Acidobacteria*, *Actinobacteria*, *Bacteroidetes*, *Proteobacteria* and *Verrucomicrobia* phyla (Fig. S4). To relate to the analyses described in the previous sections, we chose to examine the phylum- to species-level differences by classifying each of 4257 observed OTUs based on a 0.05 distance. Between 2% and 6% of these displayed statistically significant differences in abundance in pairwise sample comparisons using an independent implementation of the statistical tests employed by the RDP Library Compare tool (Wang *et al*., 2007). The OTUs that significantly changed between treatments were classified via both the RDP and Greengenes classifiers (DeSantis *et al*., 2006a; Wang *et al*., 2007). Given the short region analysed, between 6% and 20% of the OTUs could not be reliably classified by either of these methods and most of these were from the mineral samples.

By this analysis, five phyla were at least fourfold more abundant in a comparison of organic (*Bacteroidetes* and *Cyanobacteria*) and mineral horizons (*Firmicutes*, *Gemmatimonas* and *Thermotogae*) from unfertilized control samples suggesting a broad segregation of microbial groups between these soil horizons. As expected from the

statistical evaluations, comparing HFO and HCO samples revealed significant differences: decreases in the *Firmicutes* phylum and a greater than fourfold increase in the *Proteobacteria* in the HFO sample. There were no large differences in the abundances of phyla between the replicate organic samples from the same two cores, except for an overall decrease in the *Verrucomicrobia* in the GS-FLX data set (data not shown). There were some significant differences in the OTUs between the long-term control and fertilized mineral samples. For example, in the fertilized mineral sample a 17-fold increase and a 29-fold decrease was observed in the frequency of some OTUs within the *Actinobacteria* and *Firmicutes* phyla, respectively, compared with the control sample (Table 2).

Examining finer taxonomic divisions revealed differences at the class, order and family levels (Fig. 3, Table 2). At the class level, OTUs identified as *Gammaproteobacteria* were increased 10-fold in control organic versus mineral, eightfold in long-term fertilized mineral versus control, and a striking 209-fold in the long-term fertilized organic versus control (Table 2). The dramatic *Gammaproteobacteria* increase was also observed in the replicate long-term fertilized versus control organic samples analysed by GS-FLX sequencing. More variable results were observed with the *Alphaproteobacteria* and *Betaproteobacteria*; the long-term historical organic GS-FLX samples were not as different as the corresponding GS-20 samples (Table 2). At the order level, the long-term fertilized organic samples contained significantly less *Sphingobacteriales* OTUs and more OTUs corresponding to *Rhodospirillales* and *Xanthomonadales* compared with the controls (Fig. 3, Table 2). The differences in *Rhodospirillales* and *Xanthomonadales* orders were attributable to the families *Acetobacteraceae* and *Xanthomonadaceae* respectively (data not shown). Hierarchical clustering using Bray-Curtis distances based on relative abundance of orders clearly separated the long-term fertilized samples into a separate group (Fig. 3, *x*-axis dendogram). Otherwise, the mineral and organic samples clustered together similar to the diversity analyses above (Fig. 2).

As the *Acidobacteriaceae* was the dominant order across all samples, the structure of this group across samples was examined in more detail (Fig. 4, Table 2). The *Acidobacteria* phylum is presently divided into 26 subdivisions or subgroups, which in the RDP taxonomic hierarchy are considered genera. Most of these groups do not have representative isolates (Barns *et al*., 2007; Cole *et al*., 2009). There were less *Acidobacteriaceae* genera in long-term fertilized organic samples; this is reflected in the decrease in relative abundance of *Acidobacteria* in these treatments compared with other samples (Fig. 4, Fig. S4). Both acidobacterial groups 2 and 3 were present at $> 7\%$ in all samples except for the long-term fertilized samples (HFO, HFO-FLX). These changes were significant, resulting in decreases in the groups of between 6- and 127-fold in the long-term fertilized samples compared with their controls (Table 2). Similar decreases were also observed in the long-term fertilized mineral sample compared with the control, with threefold and ninefold decreases of acidobacterial groups 2 and 3 respectively. Group 6 was more abundant in the mineral (2–8% of all sequences) than in the organic samples ($< 1\%$ of all sequences) (Fig. 4), Groups 7, 15 and 16 were significantly more abundant in the mineral samples compared with the organic (Table 2). Unlike Bray-Curtis clustering based on bacterial orders (Fig. 3), the clusters based on the normalized abundances of *Acidobacteriaceae* subgroups produced four major clusters: HFO/HFO2, NFO2/NCO2/HCO2, NFO/HCO/NCO/HCM and NFM/HFM and one outlier, NCM (Fig. 4). The clustering did, however, clearly distinguish the long-term fertilized organic samples from the rest.

Beyond the trends noted in the *Acidobacteriaceae*, all analyses above detected a dramatic increase of OTUs within the *Gammaproteobacteria* allied with *Dyella*/*Rhodanobacter* species within the *Xanthomonadales*/*Xanthomonadaceae* in long-term fertilized organic soils, with significant increases ranging from 39- to 137-fold (Fig. 5, Table 2). The total number of *Dyella* and *Rhodanobacter* OTUs at the 0.05 distance level were 32 and 10 respectively. The significant changes resulted from only two OTUs affiliated with *Dyella* and two OTUs affiliated with *Rhodanobacter* from each long-term fertilized sample, where each OTU contributed between 1.1% and 6.8% of the entire population. The OTUs were not identical between samples, even within a single species (data not shown). No other OTUs from these two species comprised more than 0.5% of the population within a sample. Oligonucleotide primers specific for *Dyella* spp. were designed based on database sequences and those recovered in the GS-20 data set. These primers were used in qPCR experiments to quantify this group in duplicates of the sequenced samples and additional samples intermediate within the time series (LFO, 1989 time point). In the HFO sample, tag sequencing and qPCR agreed very well and the qPCR results were generally much greater in the long-term fertilized treatments compared with the control or short-term treatments (Fig. 5). The PCR products from these primers were sequenced from one HFO sample, and all matched the *Dyella* spp. found in that sample. However, qPCR detected increases in *Dyella*-affiliated OTUs in half of the fertilized plots sampled for this study, whereas large increases were observed in the *Dyella*-affiliated sequences from both long-term fertilized organic samples that were sequenced. These results suggest the primers utilized may not amplify all members of this group.

Table 2. Significantly different OTU abundances in pairwise sample comparisons (implementation of the RDP LibCompare statistic; $P < 0.001$).

Taxonomic rank	Name	% of OTUs		Fold increase	Fold decrease	% of OTUs		Fold increase	Fold decrease	% of OTUs		Fold increase	Fold decrease	% of OTUs		Fold increase	Fold decrease
		Org	Min			HFM	HCM			HFO	HCO			HFO_F	HCO_F		
Phylum	*Acidobacteria*	50.6	32.2	1.6		10.2	5.4	1.9		10.9	10.7	1.0		27.1	26.0	1.0	
Genus	Gp1	44.1	23.1	1.9		8.4	1.8	**4.6**		10.7	8.4	1.3		26.9	6.4	**4.2**	
Genus	Gp2	4.4	2.7	1.6		0.8	2.4		3.2	**0.1**	1.7		**16.7**	**0.1**	12.7		**127.0**
Genus	Gp3	1.7	1.3	1.4		0.1	1.0		**9.0**	**0.1**	0.6		**6.1**	0.1	6.9		**55.2**
Genus	Gp7	0.1	2.9		**52.2**	0.9	0.2	**5.3**									
Genus	Gp15	0.1	1.4		**12.5**												
Genus	Gp16	0.1	0.7		**6.5**												
Phylum	*Actinobacteria*	8.7	11.8		1.4	2.0	0.1	**17.4**						6.5	0.7	**8.8**	
Phylum	*Bacteroidetes*	3.3	**0.1**	**33.3**						2.3	0.9	2.6		**0.1**	4.4		**44.4**
Order	*Flavobacteriales*									2.3	**0.1**	**23.1**					
Order	*Sphingobacteriales*									0.1	0.9		**8.9**	**0.1**	4.4		**44.4**
Phylum	*Cyanobacteria*	1.5	**0.1**	**14.7**						**0.1**	1.3		**13.3**				
Phylum	*Firmicutes*	**0.1**	0.6		**5.5**	0.2	4.8		**29.4**								
Phylum	*Gemmatimonas*	0.2	1.1		**4.9**												
Phylum	*Proteobacteria*	29.9	32.8		1.1	7.4	5.6	1.3		37.9	7.2	**5.3**		19.8	6.0	3.3	
Class	*Alphaproteobacteria*	15.0	12.6	1.2						14.8	1.4	**10.2**		4.3	3.9	1.1	
Order	*Rhizobiales*									6.0	1.2	**4.9**					
Order	*Rhodospirillales*									5.4	0.2	**32.5**		4.3	2.0	2.1	
Family	*Acetobacteraceae*																
Class	*Betaproteobacteria*	9.1	19.6		2.2	6.4	5.5	1.2		**0.1**	4.3		**42.8**				
Class	*Gammaproteobacteria*	5.8	0.6	**10.5**		1.0	0.1	**8.5**		11.6	0.1	**208.9**		11.2	**0.1**	**112.0**	
Order	*Xanthomonadales*									11.6	0.1	**208.9**		11.2	**0.1**	**112.0**	
Genus	*Dylella*									7.7	0.1	**137.7**		7.9	**0.1**	**79.5**	
Genus	*Rhodanobacter*									3.9	**0.1**	**38.9**		3.9	**0.1**	**38.9**	
Phylum	*Thermotogae*	0.2	4.4		**25.7**												
Phylum	*Verrucomicrobia*	1.4	0.6	2.2													

Only taxa comprising > 0.5% of the community in one of the two samples being compared are listed. Abbreviations listed in Table 1. Bold/underline indicates fold changes greater than 4. Bold indicates fold calculations were based on change of abundance from 0 to 0.1 in sample.

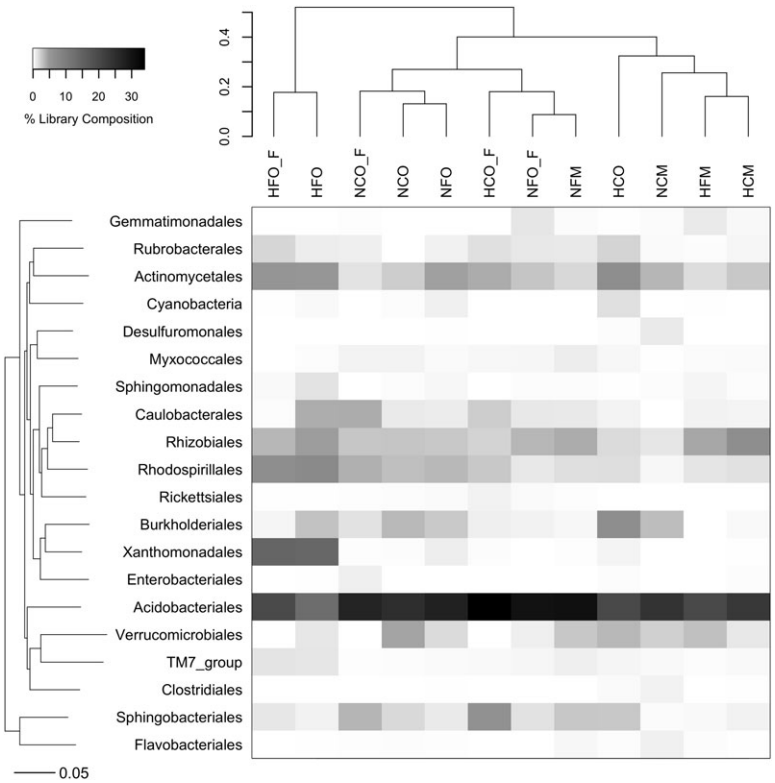

Fig. 3. Intra- and inter-sample order-level clusters with their corresponding phylogenetic affiliation. Clusters based on binned sequences from RDP classifier results. Sample communities were clustered with a Bray-Curtis similarity measurement based on relative abundance data of each order. The dendogram on the *y*-axis is a phylogram derived from full-length 16S rRNA gene sequences of representatives from each order and therefore represents phylogenetic similarity between orders. Abbreviations are listed in Table 1. The letter F indicates GS-FLX sequences.

Differences in community physiology

Community-level physiological profiling was used to examine functional changes in Toolik Lake MAT soil microbial community comparing samples from fertilized (HFO/HFM) samples with control samples (HCO/HCM). CLPP measures substrate-dependent metabolic activity in environmental samples. In total, microbes in these samples utilized 30 of 31 tested C sources, but considerable differences were observed in the pattern of substrate utilization by the different soil samples. The organic layer of control soils (HCO) utilized 27 substrates, followed by the mineral

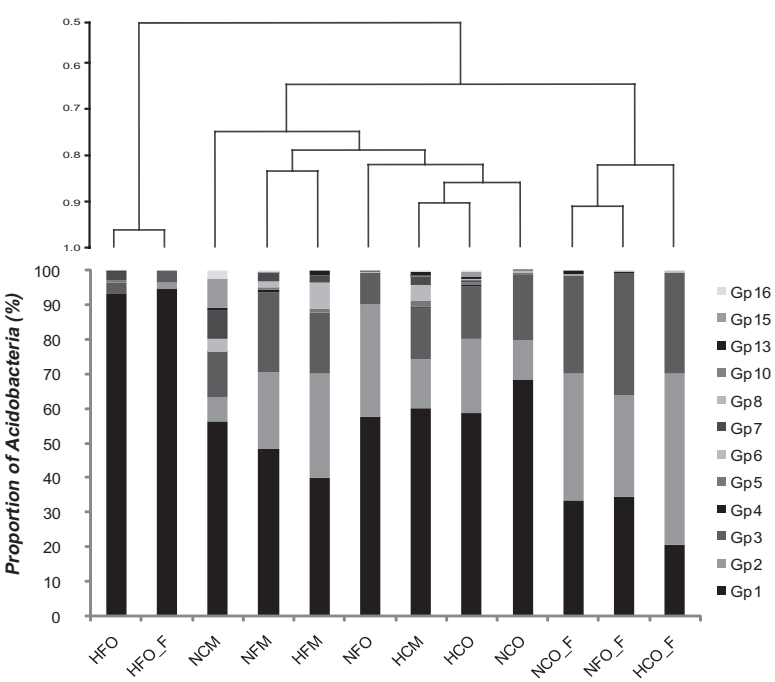

Fig. 4. Acidobacterial group similarities between MAT soil samples. Clusters based on classifications with the naive Bayesian classifier. Sample communities were clustered with a Bray-Curtis similarity measurement based on relative abundance data of each group. Abbreviations are listed in Table 1. The letter F indicates GS-FLX sequences.

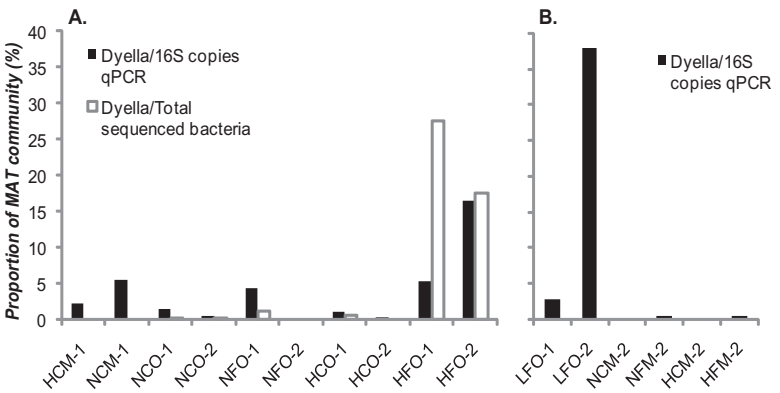

Fig. 5. Abundance of *Xanthomonadaceae* (*Dyella* spp.) in Toolik Lake moist acidic tundra soils. Measured qPCR abundances of *Dyella* spp. 16S rRNA gene copies in indicated samples, normalized to total 16S rRNA gene copies compared with percentage of *Dyella/Rhodanobacter* spp. sequences in the sequenced data sets. Intermediate time fertilized plots (LFO) were for 16 years. Numbers after sample indicate sampled core.

layers (HFM and HCM, 19 each), while the fertilized organic layer (HFO) sample only utilized 14 substrates. For substrates utilized by both the organic layers from both samples (HCO and HFO), such as mannitol and *N*-acetyl-D-glucosamine, the fertilized treatment (HFO) usually utilized it to a lesser extent (data not shown). Pairwise comparisons of CLPP data (Fig. S5) (Miguel *et al*., 2007) were used to identify compounds whose utilization significantly differed between treatments and where this difference was observed in CLPP assays of independent samples collected in 2006 and 2007 (Table 3).

Discussion

Moist acidic tundra organic soil horizons subjected to the longest fertilization treatment demonstrated the largest shifts in microbial diversity and composition, as well as differential substrate utilization patterns. In general, all mineral samples shared similar communities as measured by community membership and structure metrics, as well as at the phylum and acidobacterial group levels. The same was true for the control organic samples and short-term fertilized samples. In addition, although the replicate samples did not cluster with the original samples, perhaps due to sequencing or PCR biases, nearly identical patterns of change were observed among replicate samples of long-term fertilized organic plots.

Table 3. Substrates displaying significantly increased utilization in community-level physiological profiling (CLPP) assay of Historic plot samples.

Soil layer	Plot treatment	
	Fertilized	Control
Organic	Itaconic acid (0.0014)[a] Phenylethylamine (0.0019)	β-D-methylglucoside (0.0213)
Mineral	n.d.[b]	L-serine (0.0007)

a. Values in parentheses are *P*-values determined in two-tailed *t*-tests assuming unequal variance between samples.
b. Not detected. No substrates were differentially utilized in both years of CLPP data.

Therefore, even though MAT soils displayed a large amount of variability between samples and there were no true replicates in paired sample/sequence combinations, common and major shifts in community structure and diversity were readily observed. These patterns mirrored the previously noted plant community shifts and loss of total carbon in ecosystems subjected to long-term fertilization (Mack *et al*., 2004). This study successfully detailed major shifts and identified key bacteria that respond to nutrient additions in MAT soils. However, a more detailed temporal study would be required to correlate microbial community structure changes with plant shifts and ecosystem changes. The data presented here suggest that long-term changes result from shifts in the types of available C to the ecosystem.

Tag sequencing analyses revealed that control Arctic tundra soil microbial communities are diverse and are structured similarly to other soils (Janssen, 2006; Wallenstein *et al*., 2007). Bacterial communities in both organic and mineral horizons were predominated by *Acidobacteria* and *Proteobacteria*, followed by the *Actinobacteria* and *Bacteroidetes*. These results are similar to observations in other soils collected from Arctic, temperate and tropical soil environments (Neufeld and Mohn, 2005; Janssen, 2006; Wallenstein *et al*., 2007). However, unlike a prior study of Arctic tundra soil microbial communities (Wallenstein *et al*., 2007), significant differences were observed between the types and abundances of OTUs present either in the control organic or mineral soils, notably in the *Bacteroidetes*, *Cyanobacteria* and *Thermotogae* phyla. These differences were also present at the class and family levels, especially within the *Gammaproteobacteria* and *Acidobacteriaceae*. Further disparities were observed within the *Acidobacteriaceae* subgroups between the organic and mineral soils, especially in subgroups 7, 15 and 16. There are few isolated representatives from the *Acidobacteria*; consequently, details are lacking about the ecology of this numerically dominant group in soils (Eichorst *et al*., 2007; Pankratov *et al*., 2008) or how they contribute to nutrient cycling. This study adds valuable

information about the differential distribution of *Acidobacteria* subgroups in an important acidic soil environment. In some cases, the short region analysed was not closely allied with known bacterial 16S rRNA genes, especially from the mineral samples, suggesting that MAT soils probably contain many novel types of bacteria.

While there is much debate as to the extent of microbial diversity in soils (Gans *et al*., 2005; Schloss and Handelsman, 2006b; Roesch *et al*., 2007), the number of OTUs observed in control MAT soils did not approach saturation. Rarefaction analyses suggested a much larger amount of effort would be required to approximate the total number of OTUs in MAT soils, but that was not a goal of this study. Recent simulations of microbial diversity suggest that at least 2000 and 5000 OTUs exist per gram in agricultural and Alaskan boreal forest soils, respectively, and possibly in excess of 20 000 per gram of soil (Schloss and Handelsman, 2006b; Roesch *et al*., 2007). Thus, the estimates calculated here are a lower bound on MAT soil community diversity, and indicate that many more sequences, possibly as many as 18 000 per sample (Schloss and Handelsman, 2006b), will be required to fully describe soil community diversity. Nonetheless, there was a consistent and significant decline in the numbers of OTUs in the long-term fertilized organic samples compared with control soils. Others have also noted declines in microbial diversity in agricultural and disturbed soils compared with undisturbed soils with high-throughput sequencing approaches (Neufeld and Mohn, 2005; Roesch *et al*., 2007). The results demonstrate that a relatively modest number of pyrosequencing reads can detect differences in microbial community structure between samples. This suggests that 16S tag pyrosequencing may be productively employed as a screening and monitoring tool beyond its more common application as an exhaustive, deep sampling method.

Observed structural changes between control MAT soils and long-term fertilized bacterial communities paralleled phylum-level differences detected between tussock and shrub soils by a previous study (Wallenstein *et al*., 2007). The *Acidobacteria* were lower and *Proteobacteria* higher in the long-term fertilized samples compared with shrub-dominated soils from the previous study. In this study, there were distinct abundance and phylogenetic differences between the long-term fertilized organic samples and control or newly fertilized organic samples, as evidenced by classification and OTU cluster analyses. While these differences spanned the *Acidobacteria*, *Actinobacteria* and *Proteobacteria* phyla, the largest and most consistent increases were in the *Rhodanobacter* and *Dyella* spp. in the gammaproteobacterial *Xanthomonadaceae* family. Interestingly, members of the *Xanthomonadales* were substantially increased in both disturbed tundra soils from Canada and inorganic nutrient-fertilized cropland in Georgia (Neufeld and Mohn, 2005; Jangid *et al*., 2008). These genera have been isolated from soils (Xie and Yokota, 2005; Weon *et al*., 2007) and may benefit plant growth by increasing sulfur availability via oxidation and phosphate via solubilization (Anandham *et al*., 2008). Elevated populations of these sequences were confirmed by qPCR targeting *Dyella* spp., which showed good agreement with the tag sequence data. Finally, qPCR data collected from additional samples which were fertilized for shorter periods indicated that small-scale heterogeneity between sites may also affect the observed abundance of *Dyella* species. These combined observations indicate the potential importance of the *Xanthomonadales* in the population dynamics of altered soils.

The only other consistent increase in the long-term fertilized organic samples was in the *Acetobacteraceae* family, within the *Alphaproteobacteria*. Members of this family are important in acidic fermentation reactions and may grow on complex organic compounds (Dore *et al*., 2003); they may be able to use recalcitrant forms of carbon and supply important carbon intermediates to other microorganisms in the MAT soils. Furthermore, the total percentage of *Acidobacteria* declined in the long-term fertilized samples compared with the controls. Most of the significant decreases in OTUs were found within *Acidobacteria* groups 2 and 3, again suggesting differences in the physiology of these groups that are affected by nutrient and carbon shifts. Other changes in long-term fertilized versus control samples were of lesser magnitude or not consistent between paired cores.

Measurements of community substrate utilization patterns indicated that long-term fertilization had a consistently negative effect on the diversity of substrates utilized in the organic soil horizon. This supports the notion that a specialized community has developed in the long-term fertilized soils that has shifted away from carbon sources like β-D-methylglucoside and L-serine that might be more associated with easily degraded carbon, to those like itaconic acid and phenylethylamine that are more oxidized and aromatic in character. It should be noted that these carbon sources were significantly altered in 2 years of sampling and so likely represent consistent trends that are less prone to seasonal and site-dependent variations in microbial community activity. However, the current data set does not directly link increased population sizes and specific patterns in substrate utilization.

Conclusions

This work has refined our understanding of the impacts of experimental fertilization on MAT soils and allows us to propose the following conceptual model of how increases in N may affect this system. In the short term (0–5 years), N addition relieves N limitation and will increase microbial

extracellular enzyme production and cellular growth. These factors will increase rates of soil organic carbon (SOC) decomposition and result in amplification of lineages within predominant populations able to rapidly exploit N-limitation relief and utilize standing SOC pools (e.g. r- strategists). Over the long term (5–20 years), initially amplified subpopulations will deplete relatively labile standing SOC pools and the quality of plant inputs will decrease due to a shift towards shrub dominance. Therefore, a succession will be observed towards populations utilizing more recalcitrant fractions of SOC eventually culminating in the decreased community diversity and altered structure and metabolic patterns observed in long-term manipulated plots. Directly testing this model in relation to climate change processes and other disturbances will require significant additional experimentation and deep sequencing in this system coupled to stable isotope probing, FISH-SIMS, Micro-FISH, and the culturing of relevant microorganisms to further define how microbial community structure and metabolism affect nutrient dynamics in this ecosystem and the interplay with above-ground plant communities.

Experimental procedures

Study sites, soil collection and DNA extraction

Soil cores were taken from plots at the long-term ecological research (LTER) site at Toolik Lake, AK, USA, during August 2005 and June 2006. These plots included control and N+P-fertilized plots from experiments started in 1981, 1989 and 2005 (Mack *et al*., 2004; Nowinski *et al*., 2008). At least two cores were taken from separate plots from each experimental treatment ($n = 4$). The soils were separated into horizons (0–5 cm organic, 5–15 cm organic, 15+ organic, 0–5 mineral, and 5+ mineral to the permafrost surface) on site and placed on ice (frozen at −80°C within 1 h of collection). DNA was extracted from ~0.25 g of thoroughly mixed individual soil horizons with a MoBio Powersoil DNA extraction kit. Therefore, two of four replicate plot cores were sampled from each treatment/control and each core was separated into organic and mineral samples, for a total of 32 samples, 12 of which were used for sequence analyses.

Amplicon generation, sequencing and tag selection

The V3 region of the 16S rRNA gene was amplified from eight samples collected from the 1981 and 2005 experiments with oligonucleotide primers 338F-454A 5′-GCCTCCCTCGCGCCATCAGACTCCTACGGGAGGCAGC-3′ and 519R-454B 5′-GCCTTGCCAGCCCGCTCAGGWATTACCGCGGCKGCTG-3′, which contain the 454 Life Sciences A and B sequencing adapters (underlined). Amplicons were produced with Takara ExTaq in four to eight independent reactions from 10 ng of DNA; 0.05 μM each primer; 1.5 mM $MgCl_2$; in 25 cycles and purified using the AMPure Bead Purification kit, pooled, quantified (Picogreen assay, Invitrogen), and shipped to 454 Life Sciences. Sequencing with both A and B primers on a 16-zone plate was as previously described (Sogin *et al*., 2006). A second set of sequences were obtained from replicate cores of four treatments (NCO, NFO, HCO and HFO, Table 1). These were subjected to a tag sequencing approach (Huber *et al*., 2007) and sequenced on a 454 GS-GS-FLX machine by MWG Biosciences. Four barcoded primers were used in place of the 338F-454A primer above. Ten base pair tags (ACGAGTGCGT, ACGCTCGACA, AGACGCACTC, AGCACTGTAG) were inserted between the linker and the V3F primer. Amplifications were modified to decrease primer-dimer formation by the addition of a touchdown protocol, with the annealing temperature started at 65°C and decreased by 1°C per cycle for the first 10 cycles, followed by cycling as above.

GS-20 B read sequences were sorted by primer sequence using appropriate commands in the updated DOTUR/SONS program, MOTHUR (http://www.mothur.org/wiki/Main_Page) (Schloss and Handelsman, 2005; 2006a; Schloss *et al*., 2009); those that did not match the primer sequence were less than 100 bp or greater than 150 bp (including the primer sequence), or that contained any ambiguities (Ns) were excluded from further analysis. The GS-FLX sequences were similarly screened by primer and barcode match, ambiguities (0 or 1 N allowed) and length (between 185 and 280 bp, including the tag and primer sequence). The size range was chosen based on natural breakpoints within the GS-FLX sequence lengths. All 20 909 trimmed sequences are available at the following URL (http://www.ceoe.udel.edu/CEG/pages/resources.shtml#seqdat) as a fasta file, with a separate tab-delimitated file of sequence name and sample identifier. Representative OTU sequences from the 0.05 furthest distance calculation were deposited in GenBank and given the Accession No. GU339540–GU343711.

Diversity analyses

All sequences were combined into a single file and ordered in the forward direction and dereplicated in MOTHUR (Schloss and Handelsman, 2005; 2006a; Schloss *et al*., 2009). The dereplicated sequences were aligned using the GreenGenes NAST alignment template in MOTHUR and 55 unaligned sequences were removed (DeSantis *et al*., 2006b). The alignment was trimmed to the size of the shorter GS-20 sequences, a final average size of 106 ± 11.9 bp. A distance matrix was constructed and processed in MOTHUR. Rarefaction values, Shannon indices and several non-parametric estimates of species richness (e.g. ACE and Chao1) generated in MOTHUR were imported into Microsoft Excel for generation of diversity curves. Intra- and inter-sample diversity comparisons were analysed using Jest, Sorclass, Jabund and θ_{YC} values obtained via the updated SONS program, found in MOTHUR (Schloss and Handelsman, 2006a; Schloss *et al*., 2009).

Phylogenetic assignment of sequence tags

Each sequence was assessed phylogenetically by two independent means. To test the ability of different classifiers to correctly identify sequences based on the short V3 region, sequences assigned to the *Acidobacteria* phylum from both the RDP database (75 random sequences) and Greengenes database (540 sequences) were downloaded for analysis.

Alignments were trimmed to include only the comparable short V3 region (average 123 bp) analysed with our data set. Dereplicated sequences were classified into taxonomic groups using the naïve Bayesian classifier at a confidence threshold of 70% (Wang *et al*., 2007; Cole *et al*., 2009). Second, the sequences were aligned using the NAST sequence aligner against the prokMSA data set (DeSantis *et al*., 2006b). Then the Greengenes classifier was used to assign taxonomic identifiers to sequences analysed with Simrank to identify nearest neighbours (DeSantis *et al*., 2006a). Three separate taxon nomenclatures were used (RDP, NCBI and Hugenholtz). The naïve Bayesian classifier gave a much higher percentage of correct calls within the *Acidobacteria* phylum given the short V3 region analysed. Seventy-eight per cent of the sequences were identified as *Acidobacteria* given a confidence threshold of 70%, and this increased to 93% with no threshold, whereas the Greengenes classifier only identified 43% within the correct phylum, at any threshold. Therefore, the MAT sequences, which contain large amounts of *Acidobacteria*, were primarily assigned taxonomic groupings based on this classifier (Wang *et al*., 2007).

Comparative phylogenetic assessments

Significant shifts in 95% OTU abundance between samples were determined in a pairwise fashion by an independent implementation of the statistics used by the RDP LibCompare tool (Wang *et al*., 2007). Briefly, the statistical test of Audic and Claverie (1997) was utilized for comparisons where a given OTU had relatively low abundance in both libraries (< 5% library composition) and the standard two-population proportions test (Christensen, 1992) was used in all other instances. Statistically significant results were considered to have a *P*-value less than 0.001 (*P*-values for two-population proportions test were inferred from the *Z* critical value). The *Acidobacteria* were analysed by comparing normalized frequencies of assigned taxonomic OTUs via the RDP classifier (Cole *et al*., 2009) and using these values to perform hierarchical Bray-Curtis clustering in PAST (Hammer *et al*., 2001).

Heat mapping

Taxonomic placement of sequences was determined using the RDP Classifier tool (70% confidence) (Wang *et al*., 2007). Relative abundance of each order-level taxonomy served as input for the R PhyloTemp function (a phylogenetically enabled adaptation of the heatmap.2 function; R gplots package; http://phylotemp.microeco.org) (S.W. Polson, unpublished). The resulting heat map displays relative abundance of each order-level assignment across the individual libraries, with a phylogenetic clustering of orders along the *y*-axis and hierarchical clustering (Bray-Curtis) of relative abundance data on the *x*-axis.

Quantitative PCR

Sequences related to *Dyella* spp. group in samples were quantified using primers 338F and *Dyella* spp. R (5′-TATTCCTCRGGTACCGTCAGCC-3′), which was designed based on the GS-20 454 data set and highly related sequences in GenBank. Total bacterial 16 rRNA gene quantification was performed on the 1981, 1989 and 2005 experimental samples as described elsewhere (Suzuki *et al*., 2000). Quadruplicate reactions containing 100 pg of sample DNA in a final volume of 12.5 µl were amplified with Stratagene SYBR green mix on an ABI 7500 as follows: 95°C 10 min; 35 cycles of amplification at 95°C for 15 s and 65°C annealing temperature for 2 min, with a final dissociation step. Standard curves produced from linearized plasmid clones of target sequences were linear from 10^1 to 10^6 copies per rxn and average amplification efficiencies were 87% for bacterial 16S rRNA gene and 88% for *Dyella* spp.-specific 16S rRNA gene. Twelve clones from a *Dyella*-specific qPCR reaction from the HFO sample were sequenced and their closest BLAST matches were to *Dyella* spp.

Community-level physiological profiling

Composited soil samples from organic and mineral layers of new and historical plots were used to make 1:10 (w/v) slurries, which were transported to the University of Delaware for CLPP analysis using BIOLOG EcoPlates in 2006 or analysed on site in 2007. A total dilution of 1:5000 (w/v) where soil particles were not allowed to settle during dilution (Waldrop *et al*., 2000) incubated at room temperature for less than 72 h yielded reproducible results, whereas frozen soil samples, 4°C incubations and long-term incubations were irreproducible (data not shown). Each sample was analysed in triplicate (three dilutions of the original slurry) in a single BIOLOG EcoPlate. Colour development (A_{595}) was measured using a plate reader. Data were transferred to Microsoft Excel to correct for initial absorbance in each well, calculate average well colour development (AWCD), well absorbance/AWCD (Waldrop *et al*., 2000), and plot well absorbance over time for any given substrate.

Acknowledgements

We gratefully acknowledge G. Shaver, S. Bret-Harte and J. Laundre for maintaining the Toolik Lake LTER plots and facilitating sampling; J. DeMarco and M. Kokes for sampling; M. Cottrell for computer programming; and L. Rejto and B. Su of the UD StatLab for R script development, and Thermo-Fisher Scientific for the loan of a plate reader to use at Toolik Lake in 2007. This work was supported by an NSF SGER grant (DEB 0542283) to B.J.C. and T.E.H.

References

Anandham, R., Gandhi, P.I., Madhaiyan, M., and Sa, T. (2008) Potential plant growth promoting traits and bioacidulation of rock phosphate by thiosulfate oxidizing bacteria isolated from crop plants. *J Basic Microbiol* **48:** 439–447.

Audic, S., and Claverie, J.M. (1997) The significance of digital gene expression profiles. *Genome Res* **7:** 986–995.

Barns, S.M., Cain, E.C., Sommerville, L., and Kuske, C.R. (2007) *Acidobacteria* phylum sequences in uranium-contaminated subsurface sediments greatly expand the known diversity within the phylum. *Appl Environ Microbiol* **73:** 3113–3116.

Chapin, F.S., and Shaver, G.R. (1988) Differences in carbon and nutrient fractions among Arctic growth forms. *Oecologia* **77:** 506–514.

Chapin, F.S., Shaver, G.R., Giblin, A.E., Nadelhoffer, K.J., and Laundre, J.A. (1995) Responses of Arctic tundra to experimental and observed changes in climate. *Ecology* **76:** 694–711.

Christensen, H.B. (1992) *Introduction to Statistics: A Calculus-Based Approach*. Orlando, FL, USA: Harcourt Brace Jovanovich.

Cole, J.R., Wang, Q., Cardenas, E., Fish, J., Chai, B., Farris, R.J., *et al.* (2009) The Ribosomal Database Project: improved alignments and new tools for rRNA analysis. *Nucleic Acids Res* **37:** D141–D145.

DeSantis, T.Z., Hugenholtz, P., Larsen, N., Rojas, M., Brodie, E.L., Keller, K., *et al.* (2006a) Greengenes, a chimera-checked 16S rRNA gene database and workbench compatible with ARB. *Appl Environ Microbiol* **72:** 5069–5072.

DeSantis, T.Z., Hugenholtz, P., Keller, K., Brodie, E.L., Larsen, N., Piceno, Y.M., *et al.* (2006b) NAST: a multiple sequence alignment server for comparative analysis of 16S rRNA genes. *Nucleic Acids Res* **34:** W394–W399.

Deslippe, J.R., Egger, K.N., and Henry, G.H.R. (2005) Impacts of warming and fertilization on nitrogen-fixing microbial communities in the Canadian high Arctic. *FEMS Microbiol Ecol* **53:** 41–50.

Dixon, R.K., Brown, S., Houghton, R.A., Solomon, A.M., Trexler, M.C., and Wisniewski, J. (1994) Carbon pools and flux of global forest ecosystems. *Science* **263:** 185.

Dore, S.Y., Clancy, Q.E., Rylee, S.M., and Kulpa, C.F. (2003) Naphthalene-utilizing and mercury-resistant bacteria isolated from an acidic environment. *Appl Microbiol Biotechnol* **63:** 194–199.

Eckburg, P.B., Bik, E.M., Bernstein, C.N., Purdom, E., Dethlefsen, L., Sargent, M., *et al.* (2005) Diversity of the human intestinal microbial flora. *Science* **308:** 1635–1638.

Eichorst, S.A., Breznak, J.A., and Schmidt, T.M. (2007) Isolation and characterization of soil bacteria that define *Teniglobus* gen. nov., in the phylum *Acidobacteria*. *Appl Environ Microbiol* **73:** 2708–2717.

Fierer, N., and Jackson, R.B. (2006) The diversity and biogeography of soil bacterial communities. *Proc Natl Acad Sci USA* **103:** 626–631.

Fulthorpe, R.R., Roesch, L.F.W., Riva, A., and Triplett, E.W. (2008) Distantly sampled soils carry few species in common. *ISME J* **2:** 901–910.

Gans, J., Wolinsky, M., and Dunbar, J. (2005) Computational improvements reveal great bacterial diversity and high metal toxicity in soil. *Science* **309:** 1387–1390.

Ge, Y., Zhang, J.B., Zhang, L.M., Yang, M., and He, J.Z. (2008) Long-term fertilization regimes and diversity of an agricultural affect bacterial community structure soil in northern China. *J Soils Sediments* **8:** 43–50.

Goulden, M.L., Wofsy, S.C., Harden, J.W., Trumbore, S.E., Crill, P.M., Gower, S.T., *et al.* (1998) Sensitivity of boreal forest carbon balance to soil thaw. *Science* **279:** 214–217.

Hammer, O., Harper, D.A.T., and Ryan, P.D. (2001) PAST: paleontological statistics software package for education and data analysis. *Palaeontol Electron* **4:** 9.

Hobbie, S.E., and Gough, L. (2004) Litter decomposition in moist acidic and non-acidic tundra with different glacial histories. *Oecologia* **140:** 113–124.

Houghton, R.A. (1996) Terrestrial sources and sinks of carbon inferred from terrestrial data. *Tellus B Chem Phys Meteorol* **48:** 420–432.

Huber, J.A., Welch, D.B.M., Morrison, H.G., Huse, S.M., Neal, P.R., Butterfield, D.A., and Sogin, M.L. (2007) Microbial population structures in the deep marine biosphere. *Science* **318:** 97–100.

Huse, S.M., Huber, J.A., Morrison, H.G., Sogin, M.L., and Welch, D.M. (2007) Accuracy and quality of massively parallel DNA pyrosequencing. *Genome Biol* **8:** R143.

Jangid, K., Williams, M.A., Franzluebbers, A.J., Sanderlin, J.S., Reeves, J.H., Jenkins, M.B., *et al.* (2008) Relative impacts of land-use, management intensity and fertilization upon soil microbial community structure in agricultural systems. *Soil Biol Biochem* **40:** 2843–2853.

Janssen, P.H. (2006) Identifying the dominant soil bacterial taxa in libraries of 16S rRNA and 16S rRNA genes. *Appl Environ Microbiol* **72:** 1719–1728.

McCaig, A.E., Glover, L.A., and Prosser, J.I. (1999) Molecular analysis of bacterial community structure and diversity in unimproved and improved upland grass pastures. *Appl Environ Microbiol* **65:** 1721–1730.

Mack, M.C., Schuur, E.A.G., Bret-Harte, M.S., Shaver, G.R., and Chapin, F.S. (2004) Ecosystem carbon storage in arctic tundra reduced by long-term nutrient fertilization. *Nature* **431:** 440–443.

McKenna, P., Hoffmann, C., Minkah, N., Aye, P.P., Lackner, A., Liu, Z.Z., *et al.* (2008) The macaque gut microbiome in health, lentiviral infection, and chronic enterocolitis. *PLoS Pathog* **4:** e20. doi:10.1371/jopurnal.ppat.0040020.

Miguel, C.S., Dulinski, M., and Tate, R.L. (2007) Direct comparison of individual substrate utilization from a CLPP study: a new analysis for metabolic diversity data. *Soil Biol Biochem* **39:** 1870–1877.

Neff, J.C., and Hooper, D.U. (2002) Vegetation and climate controls on potential CO2, DOC and DON production in northern latitude soils. *Glob Chang Biol* **8:** 872–884.

Neufeld, J.D., and Mohn, W.W. (2005) Unexpectedly high bacterial diversity in arctic tundra relative to boreal forest soils, revealed by serial analysis of ribosomal sequence tags. *Appl Environ Microbiol* **71:** 5710–5718.

Nowinski, N.S., Trumbore, S.E., Schuur, E.A.G., Mack, M.C., and Shaver, G.R. (2008) Nutrient addition prompts rapid destabilization of organic matter in an arctic tundra ecosystem. *Ecosystems* **11:** 16–25.

Pankratov, T.A., Serkebaeva, Y.M., Kulichevskaya, I.S., Liesack, W., and Dedysh, S.N. (2008) Substrate-induced growth and isolation of *Acidobacteria* from acidic Sphagnum peat. *ISME J* **2:** 551–560.

Pavoine, S., Dufour, A.B., and Chessel, D. (2004) From dissimilarities among species to dissimilarities among communities: a double principal coordinate analysis. *J Theor Biol* **228:** 523–537.

Post, W.M., Emanuel, W.R., Zinke, P.J., and Stangenberger, A.G. (1982) Soil carbon pools and world life zones. *Nature* **298:** 156–159.

Quince, C., Lanzen, A., Curtis, T.P., Davenport, R.J., Hall, N., Head, I.M., *et al.* (2009) Accurate determination of

microbial diversity from 454 pyrosequencing data. *Nat Methods* **6:** 639–U627.
Roesch, L.F., Fulthorpe, R.R., Riva, A., Casella, G., Hadwin, A.K.M., Kent, A.D., *et al.* (2007) Pyrosequencing enumerates and contrasts soil microbial diversity. *ISME J* **1:** 283–290.
Schimel, J.P., and Weintraub, M.N. (2003) The implications of exoenzyme activity on microbial carbon and nitrogen limitation in soil: a theoretical model. *Soil Biol Biochem* **35:** 549–563.
Schloss, P.D., and Handelsman, J. (2005) Introducing DOTUR, a computer program for defining operational taxonomic units and estimating species richness. *Appl Environ Microbiol* **71:** 1501–1506.
Schloss, P.D., and Handelsman, J. (2006a) Introducing SONS, a tool for operational taxonomic unit-based comparisons of microbial community memberships and structures. *Appl Environ Microbiol* **72:** 6773–6779.
Schloss, P.D., and Handelsman, J. (2006b) Toward a census of bacteria in soil. *PLoS Comput Biol* **2:** 786–793.
Schloss, P.D., Westcott, S.L., Ryabin, T., Hall, J.R., Hartmann, M., Hollister, E.B., *et al.* (2009) Introducing mothur: open-source, platform-independent, community-supported software for describing and comparing microbial communities. *Appl Environ Microbiol* **75:** 7537–7541.
Shaver, G.R., Bret-Harte, S.M., Jones, M.H., Johnstone, J., Gough, L., Laundre, J., and Chapin, F.S. (2001) Species composition interacts with fertilizer to control long-term change in tundra productivity. *Ecology* **82:** 3163–3181.
Sogin, M.L., Morrison, H.G., Huber, J.A., Welch, D.M., Huse, S.M., Neal, P.R., *et al.* (2006) Microbial diversity in the deep sea and the underexplored 'rare biosphere'. *Proc Natl Acad Sci USA* **103:** 12115–12120.
Stackebrandt, E., and Goebel, B.M. (1994) A place for DNA–DNA reassociation and 16S ribosomal-RNA sequence-analysis in the present species definition in bacteriology. *Int J Syst Bacteriol* **44:** 846–849.
Suzuki, M.T., Taylor, L.T., and DeLong, E.F. (2000) Quantitative analysis of small-subunit rRNA genes in mixed microbial populations via 5′-nuclease assays. *Appl Environ Microbiol* **66:** 4605–4614.
Waldrop, M.P., Balser, T.C., and Firestone, M.K. (2000) Linking microbial community composition to function in a tropical soil. *Soil Biol Biochem* **32:** 1837–1846.
Wallenstein, M.D., McMahon, S., and Schimel, J. (2007) Bacterial and fungal community structure in Arctic tundra tussock and shrub soils. *FEMS Microbiol Ecol* **59:** 428–435.
Wang, Q., Garrity, G.M., Tiedje, J.M., and Cole, J.R. (2007) Naive Bayesian classifier for rapid assignment of rRNA sequences into the new bacterial taxonomy. *Appl Environ Microbiol* **73:** 5261–5267.
Wardle, D.A., Bonner, K.I., and Nicholson, K.S. (1997) Biodiversity and plant litter: experimental evidence which does not support the view that enhanced species richness improves ecosystem function. *Oikos* **79:** 247–258.
Weintraub, M.N., and Schimel, J.P. (2005) Nitrogen cycling and the spread of shrubs control changes in the carbon balance of Arctic tundra ecosystems. *Bioscience* **55:** 551–551.
Weon, H.Y., Kim, B.Y., Hong, S.B., Jeon, Y.A., Kwon, S.W., Go, S.J., and Koo, B.S. (2007) *Rhodanobacter ginsengisoli* sp. nov. and *Rhodanobacter terrae* sp. nov., isolated from soil cultivated with Korean ginseng. *Int J Syst Evol Microbiol* **57:** 2810–2813.
Xie, C.H., and Yokota, A. (2005) *Dyella japonica* gen. nov., sp. nov. a gamma-proteobacterium isolated from soil. *Int J Syst Evol Microbiol* **55:** 753–756.

Supporting information

Additional Supporting Information may be found in the online version of this article:

Fig. S1. Rarefaction analyses of individual MAT samples, based on 0.03, 0.05 and 0.10 distances. Panels separated by soil type (mineral versus organic) or by sequence data set. F indicated replicate cores sequenced using GS-FLX technology.
Fig. S2. Shannon diversity indices of individual MAT samples, based on 0.03, 0.05 and 0.10 distances. Panels separated by soil type (mineral versus organic) or by sequence data set. F indicated replicate cores sequenced using GS-FLX technology.
Fig. S3. Non-parametric analyses (ACE, Chao1) of individual MAT samples, based on 0.05 distances. Panels separated by soil type (mineral versus organic) or by sequence data set. Low and high confidence intervals of the long-term samples (HCO, HFO, HCM, HFM) are indicated by error bars. F indicates replicate cores sequenced using GS-FLX technology.
Fig. S4. Percentages of different phyla in MAT microbial communities. Percentages based on reverse read (B) sequences. (A) Total organic and total mineral layers; (B) HCO and HFO. The RDP classifier was used to identify the 16S rRNA gene sequence taxa at a confidence threshold of 70%. The asterisk (*) indicated significance values < 0.01 using the RDP LibCompare function (70% confidence threshold).
Fig. S5. CLPP data analysis by the method of Miguel and colleagues (2007). Average well colour development data for fertilized organic soil layers (HFO) were plotted against that of control organic soil layers (HCO) from samples collected in September 2007. The average utilization of each substrate in two samples is plotted along with the standard deviation derived from replicated samples ($n = 3$–6). The dashed line indicates the function $y = x$. Substrates whose standard deviations did not overlap the 1:1 relationship were considered to be differentially utilized. Arrows indicate substrates that were differentially utilized by each sample. Only substrates that were differentially utilized in both 2006 and 2007 CLPP data sets were included in Table 3.

Please note: Wiley-Blackwell are not responsible for the content or functionality of any supporting materials supplied by the authors. Any queries (other than missing material) should be directed to the corresponding author for the article.